ELSEVIER

Neurobiology of Aging 33 (2012) 588–602

NEUROBIOLOGY OF AGING

www.elsevier.com/locate/neuaging

Human umbilical cord blood-derived mesenchymal stem cells improve neuropathology and cognitive impairment in an Alzheimer's disease mouse model through modulation of neuroinflammation

Hyun Ju Lee[a,b], Jong Kil Lee[a,c], Hyun Lee[a,b], Janet E. Carter[d], Jong Wook Chang[e], Wonil Oh[e], Yoon Sun Yang[e], Jun-Gyo Suh[f], Byoung-Hee Lee[g], Hee Kyung Jin[a,c,*], Jae-sung Bae[a,b,]

[a] *Stem Cell Neuroplasticity Research Group, Kyungpook National University, Daegu, Korea*

[b] *Department of Physiology, Cell and Matrix Research, Institute, BSEI, World, Class University Program, School of Medicine, Kyungpook National University, Daegu, Korea*

[c] *Department of Laboratory Animal Medicine, Cell and Matrix Research Institute, College of Veterinary Medicine, Kyungpook National University, Daegu, Korea*

[d] *Department of Mental Health Sciences, Royal Free and University College Medical School, University College London, London, UK*

[e] *Biomedical Research Institute, MEDIPOST Co., Ltd., Republic of Korea*

[f] *Department of Medical Genetics, College of Medicine, Hallym University, Chuncheon, Korea*

[g] *Division of Biological Resources Coordination, National Institue of Biological Resources, Incheon, Korea*

Received 1 October, 2009; received in revised form 26 March 2010; accepted 31 March 2010

Abstract

Human umbilical cord blood-derived mesenchymal stem cells (hUCB-MSC) have a potential therapeutic role in the treatment of neurological disorders, but their current clinical usage and mechanism of action has yet to be ascertained in Alzheimer's disease (AD). Here we report that hUCB-MSC transplantation into amyloid precursor protein (APP) and presenilin1 (PS1) double-transgenic mice significantly improved spatial learning and memory decline. Furthermore, amyloid-β peptide (Aβ) deposition, β-secretase 1 (BACE-1) levels, and tau hyperphosphorylation were dramatically reduced in hUCB-MSC transplanted APP/PS1 mice. Interestingly, these effects were associated with reversal of disease-associated microglial neuroinflammation, as evidenced by decreased microglia-induced proinflammatory cytokines, elevated alternatively activated microglia, and increased anti-inflammatory cytokines. These findings lead us to suggest that hUCB-MSC produced their sustained neuroprotective effect by inducing a feed-forward loop involving alternative activation of microglial neuroinflammation, thereby ameliorating disease pathophysiology and reversing the cognitive decline associated with Aβ deposition in AD mice.

Keywords: Alzheimer's disease; Human umbilical cord blood-derived mesenchymal stem cell; Amyloid-β; microglia; Spatial learning and memory; Microglial neuroinflammation

Genetic studies in familial Alzheimer's disease (AD) suggest that amyloid β-peptide (Aβ) plays a key pathogenic role in AD, and have connected the Aβ plaque with formation of intracellular tau tangles, another neurotoxic feature of AD (Huang and Jiang, 2009; Mattson, 2004). Aβ plaques are potent activators of microglia and astrocytes, 2-cell types that respond to cerebral amyloidosis by chronic proinflammatory activation (Praticò and Trojanowski, 2000). Numerous reports indicate that the neuroinflammatory process contributes to the pathogenesis of AD. Thus, therapeutic strategies aimed at manipulating this inflammatory cascade, including Aβ immunization (Games et al., 2000; Schenk et al., 1999) and modulation of microglial activation

* Corresponding authors at: Kyungpook National University, Department of Physiology, School of Medicine, 101 Dongindong 2 Ga, Jung-Gu, Daegu 700-422, Republic of Korea; College of Veterinary Medicine, Kyungpook National University, Sankyuk 3-dong, Buk-gu, Daegu 702-701, Republic of Korea. Tel.: +82 53 420 4815, 82 53 950 5966; fax: +82 53 424 3349, 82 53 950 5955.

*E-mail addresses:*jsbae@knu.ac.kr (J.-s. Bae), hkjin@knu.ac.kr (H.K. Jin).

0197-4580/$ – see front matter © 2012 Elsevier Inc. All rights reserved.
doi:10.1016/j.neurobiolaging.2010.03.024

(Tan et al., 1999), have been evaluated, and are able to reduce AD-like pathology and improve behavioral impairment in AD transgenic mouse models. Currently, however, no treatment is available for AD patients to modulate neuroinflammation and prevent the cell death that results in inevitable decline.

Administration of cells isolated from human umbilical cord has produced beneficial effects in animal models for neurodegenerative diseases, including AD, by using cell replacement or immunomodulatory strategies (Chen et al., 2006; Nikolic et al., 2008). Recent developments in stem cell technology raise the prospect of cell replacement therapy for neurodegenerative disorders. For example, human umbilical cord blood-derived mesenchymal stem cells (hUCB-MSC) are under intense investigation as a potential therapeutic source of neurons to replace damaged or lost cells in neurological diseases (Harris, 2008; Hirko et al., 2008). Cord blood cells also have been shown to antagonize proinflammatory T_h1, and stimulate anti-inflammatory T_h2 responses by immunomodulation in neurological disorders (Vendrame et al., 2005). Although hUCB-MSC have been suggested as a potential therapeutic approach for several neurological disorders (Harris, 2008; Hirko et al., 2008), the actual therapeutic impact of hUCB-MSC on AD neuropathology, especially cognitive impairments, and their mechanism of action has not yet been ascertained.

Many studies including those on the human post-mortem brain, as well as neuroimaging analysis in AD patients and in rodent transgenic models, have provided evidence that microglia are attracted to and surround senile plaques in AD (Van Groen et al., 2009; Wiley et al., 2009). However, their exact role in the pathogenesis of AD remains to be elucidated. Some studies have also indicated that Aβ can activate microglia to produce cytokines and neurotoxins, hence promoting neurodegeneration (El Khoury et al., 2003; Meda et al., 1995). In contrast, others have suggested that microglia have a neuroprotective role, secreting neurotrophic agents and eliminating toxic Aβ by phagocytosis (Jimenez et al., 2008; Simard et al., 2006). One study observed the existence of an age-dependant phenotypic change of microglial activation in the hippocampus of an AD mouse model, from an alternative (expressing IL-4) activation state to a classic cytotoxic (expressing IL-1β and TNF-α) phenotype (Jimenez et al., 2008). Interestingly, more recent work in an ischemic mouse model confirmed that microglia can switch phenotypes to become "alternatively activated" such that anti-inflammatory effects predominate, and that this is promoted by adult stem cell transplantation (Ohtaki et al., 2008). Our previous report also showed that intracerebral transplantation of bone marrow stem cells can increase microglial activation and reduce Aβ deposits in an acutely induced AD model. The activated microglia were located near the Aβ deposits, and their morphology was changed from ramified to ameboid as an action of the microglial phagocytosis (Lee et al., 2009).

Here, we examined whether hUCB-MSC transplantation into the hippocampus of an AD mouse model could have beneficial effects through microglia activation, and whether these microglia are "alternatively activated" by the immunomodulatory properties of the transplanted hUCB-MSC. We found that hUCB-MSC transplantation promoted alternative microglial activation by opposing proinflammatory and stimulating anti-inflammatory pathways, rescued cognitive impairment, and reduced Aβ deposits, β-secretase 1 (BACE-1), and tau pathology in the brain.

1. Methods

1.1. Animals

A double transgenic mouse model of AD was used for the evaluation of hUCB-MSC intracerebral transplantation. APP/PS1 double transgenic and nontransgenic mice were generated from matings between single transgenic mice expressing human mutant APP (Hsiao et al., 1996) and mutant PS1 (Duff et al., 1996). The single APP and PS1 transgenic mice were originally obtained from Taconic and Jackson Laboratory, respectively. Given the existence of gender differences in Aβ deposition in this model, we used only males in the present study. All procedures were in accordance with an animal protocol approved by the Kyungpook National University Institutional Animal Care and Use Committee (IACUC).

1.2. Isolation and culture of hUCB-MSC

Human UCB samples were collected from the umbilical vein of deliveries with informed maternal consent. In all cases, UCB harvests were processed within 24 hours of collection, with viability of more than 90%. Isolation and expansion of hUCB-MSC were performed according to our previous report (Kim et al., 2009). Differentiation characteristics of hUCB-MSC, including their ability to form osteogenic, chondrogenic, and adipogenic lineages were tested before the onset of this study.

1.3. Implantation of guide cannula

One week before the first hUCB-MSC injection, each mouse underwent surgery to implant a guide cannula into its brain (Lee et al., 2009). Detailed methodology is described in the Supplemental Methods section.

1.4. Transplantation of hUCB-MSC into the hippocampal brain region

hUCB-MSC or PBS were administered once every 2 weeks (n = 15 per group). APP/PS1 mice were treated starting at 7 months, 1 week of age, and finishing at 8 months, 1 week of age (total three times once every 2 weeks

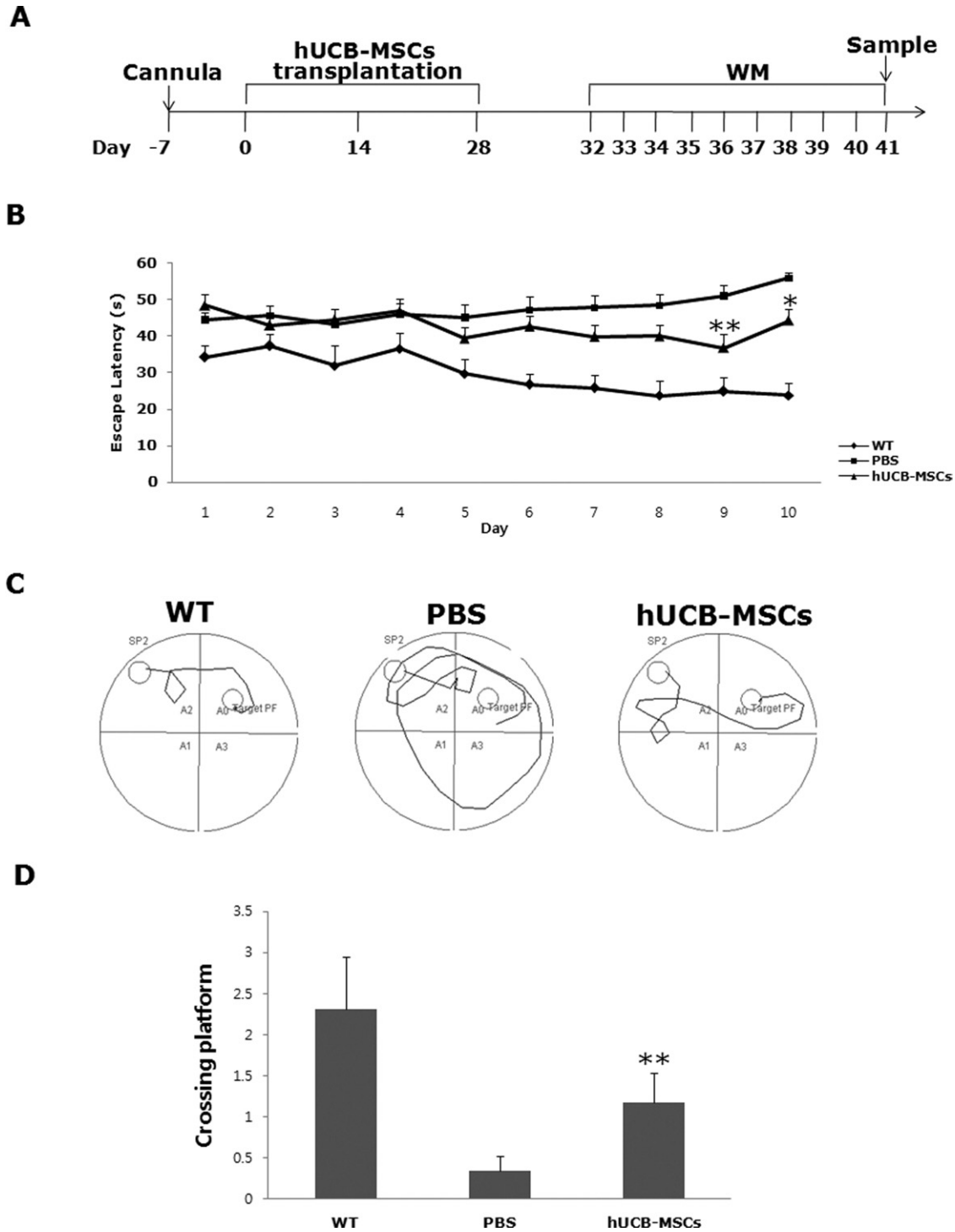

Fig. 1. Intrahippocampal hUCB-MSC transplantation improves spatial memory. (A) Experimental design for the hUCB-MSC treatment of an APP/PS1 mouse AD model. (B) Water maze escape latencies in seconds over a 10 day time period for APP/PS1 mice whose hippocampi were bilaterally injected with PBS or hUCB-MSC and WT controls. For complete test, a total of 40 sessions over 10 days were given. Graph shows average escape latencies per day for each condition. Escape latencies in the hUCB-MSC transplanted APP/PS1 group show improved learning over time ($n = 15$ for each of the three groups). (C) Representative swimming paths at Day 10 of training. (D) On the final day, spatial learning assessed after completion of training using a single probe test. Results indicate the number of times each animal entered the small target zone during the 60 second probe trial. hUCB-MSC treatment significantly rescued learning deficits compared with PBS infused APP/PS1 mice. (ANOVA, Tukey's HSD test. $*p < 0.05$ and $**p < 0.01$ compared with PBS infused mice).

by intracerebral transplantation). More information is described in Figure 1A. The tip of the injection cannula projected beyond the guide cannula by 1 mm. It was connected by flexible polyethylene tubing to the microinjection system, which housed a 25 μl Hamilton syringe. Three microliters of the cell suspension (approximately 1×10^5 cells) were injected into the hippocampus bilaterally. The cell suspension was delivered at a rate of 0.3 μl/min. For controls, 3 μl of PBS were implanted. After surgery, each mouse was kept in an individual cage to prevent the removal of the guide cannula by other animals.

1.5. Tissue preparation and thioflavin S staining

APP/PS1 mice were sacrificed after behavioral testing. The mice were anesthetized with 2.5% Avertin in PBS and immediately cardiac perfused with 4% paraformaldehyde in PBS. After perfusion, brains were excised, postfixed overnight at 4 °C, and incubated in 30% sucrose at 4 °C until equilibrated. Sequential 30 or 14 μm coronal sections were taken on a cryostat (CM30 50S; Leica) and stored at −20 °C. Brain sections were incubated for 5 minutes at a concentration of 0.5% Thioflavin S (Sigma-Aldrich) dissolved in 50% ethanol, and then washed twice with 50% ethanol for 5 minutes each and once with tap water for 5 minutes, and mounted with mounting medium.

1.6. Immunohistochemistry

The primary antibodies were 20G10 (mouse, diluted 1 : 1,000), G30 (rabbit, diluted 1 : 1,000), Iba-1 (rabbit, diluted 1 : 500, Wako), AMCase (goat, diluted 1 : 100, Santa Cruz), IL-4 (goat, diluted 1 : 250, Santa Cruz), α-smooth muscle actin (α-SM, diluted 1 : 400, Sigma-Aldrich), IL-1β (goat, diluted 1 : 10, R&D), TNF-α (goat, diluted 1 : 20, R&D), and AT8 (rabbit, diluted 1 : 500, Pierce). For visualization, the primary antibody was developed by incubating with Alexa Fluor 488-, 546-, 594- or 633-conjugated secondary antibodies for 1 hour at RT or by incubating with biotinylated secondary antibodies against the corresponding species. This was followed by BCIP/NBT (Vector Laboratories) or DAB (Vector Laboratories) using the instructions of the manufacturer for alkaline phosphatase or peroxidase labeling. For double fluorescence labeling of Aβ and microglia, the brain sections were stained with 0.5% Thioflavin S, and then stained with primary antibodies as described above. In some experiments, after primary antibody staining of IL-1β (1 : 10), TNF-α (1 : 20) and IL-4 (1 : 250), tissue sections were incubated overnight at 4 °C with secondary primary antibody (Iba-1, 1 : 500). The sections were analyzed with a laser scanning confocal microscope equipped with Fluoview FV1000 imaging software (Olympus FV1000, Japan) or by use of Olympus BX51 microscope.

1.7. Western blot analysis

Brains were isolated from mice after behavioral testing. The brain tissues were weighed and sonicated in 10× volume of RIPA buffer (20 mM Tris, pH 7.4, 150 mM NaCl, 1% NP-40, 2 mM EDTA, 0.1% Na deoxycholate, 0.1% SDS, 50 mM NaF, 1 mM PMSF, 1 mM Na_3VO_4, 10 μg mL^{-1} aprotinin and 10 μg/mL leupeptin) plus protease inhibitors. Protein concentrations were determined using the Bradford technique (Bio-Rad, Hercules, CA). Western blots were carried out using extracts from different brain regions (cerebral cortex, hippocampus) extracts, and equal amounts of protein were separated on 12% SDS-PAGE and transferred to PVDF membranes. Immunoblotting was carried out with antibodies against 6E10 (1 : 500 dilution; Signet), and β-actin (1 : 500 dilution; Santa Cruz). Western blots were developed using enhanced chemiluminescence (Amersham Biosciences).

1.8. Aβ ELISA

Aβ 40 (KHB3481) and Aβ 42 (KHB3441) were assayed using fluorescent-based ELISA kits (Invitrogen, Camarillo, CA) and appropriate Aβ standards, according to the manufacturer's protocol. The hippocampus and frontal cortex from one hemisphere were homogenized in guanidine buffer with a final concentration of 50 mM Tris and 5 M guanidine HCl, pH 8.0. Homogenates were mixed in RT for 3–4 hrs. After mixing, homogenates were diluted in PBS containing 5% BSA, 0.03% Tween 20, and a protease inhibitor cocktail (Calbiochem). Samples were pipetted into a monoclonal antibody (NH2-terminus of Human Aβ) precoated wells, and then coincubated with rabbit antibody specific for the Aβ 40 or 42. Each Aβ standard and experimental sample was run in duplicate and the results were averaged.

1.9. Quantitative real-time PCR

Total RNA was isolated from frontal cortex and hippocampus from WT and APP/PS1 mice. RNA extraction was performed with the RNeasy Lipid Tissue Mini kit (Qiagen, Korea, Ltd) according to the manufacturer's instructions. The RNA samples from three individual animals per group in the different experiments were used to prepare cDNA for RT-PCR using the oligo$(dT)_{12\text{-}18}$ primers and SuperScript III RT (Invitrogen). the cDNA was quantified using the QuantiTect SYBR Green PCR Kit (Qiagen, Korea, Ltd). The PCR Primers used are described in a supplemental Table. Each reaction was performed in a volume of 20 μl that contained 100 ng cDNA, 10 μl SYBR Green PCR Master Mix and 5 pM of each (Forward and reverse) PCR primer. The 20 μl of total mixture was placed in the 0.1 ml tube. Quantitative real-time PCR was performed using a Corbett Rotor-Gene 6000 quantitative PCR system (Corbett Life Sciences, Sydney, Australia) with the following cycling parameters: 95 °C for 15 minutes followed by 40 cycles of 95 °C for 30 seconds, 58 °C for 30 seconds, 72 °C for 30 seconds, followed by amplicon dissociation (95 °C for 1 minute, 50 °C for 45 seconds, increasing at 0.5 °C/cycle until 95 °C was reached). All reactions were per-

formed in triplicate. Gene expression results were calculated using the delta delta cycle threshold (two delta delta CT) method (Livak and Schmittgen, 2001). The two delta delta CT method was used to determine mean fold changes in gene expression between the control and target genes. The results were normalized using β-actin, 18S rRNA and GAPDH expression.

1.10. Behavioral testing

We used the Morris water maze task to assess hippocampal-dependent spatial memory performance (Morris et al., 1982). Detailed methodology is described in the Supplemental Methods section.

1.11. Statistical analysis

The Student's *t*-test was used to compare two groups, whereas the Tukey's HSD test and Repeated Measures analysis of variance test was used for multigroup comparisons according to the SAS statistical package (release 9.1; SAS Institute, Inc., Cary, NC). $p < 0.05$ was considered significant.

2. Results

2.1. hUCB-MSC transplantation improves cognitive impairments in APP/PS1 mice

To assess whether hUCB-MSC could improve spatial learning and memory in a transgenic AD mice, PBS and hUCB-MSC treated male APP/PS1 mice and their control (PBS injected) and WT littermates were tested at 4 days after the last hUCB-MSC treatment in the hidden platform version of the Morris water maze test (Morris et al., 1982). Analysis was begun after the final of three injections of hUCB-MSC (once every 2 weeks by intracerebral injection), and water maze testing was carried out for 10 consecutive days. The complete protocol is summarized (Fig. 1A). The PBS infused APP/PS1 mice exhibited significantly impaired learning/memory compared with PBS infused WT mice in the water maze test. However, we found that APP/PS1 mice transplanted with hUCB-MSC performed significantly better on the water maze test than PBS infused counterparts ($p < 0.01$; Fig. 1B). Representative navigation paths at Day 10 of training provided evidence that spatial learning acquisition was impaired in the APP/PS1 mice that received PBS relative to animals injected with hUCB-MSC, who displayed a navigation pattern similar to control animals (Fig. 1C). On the final day, a single probe test was performed in which the platform was removed to assess whether the animals used a nonspatial strategy to find the platform. During the probe trial, we calculated the number of times each animal entered the small target zone during the 60 second test. The deficits in the PBS infused APP/PS1 mice were significantly improved in the hUCB-MSC treated mice ($p < 0.01$; Fig. 1D).

2.2. hUCB-MSC can reduce total Aβ load and tau hyperphosphorylation in APP/PS1 mice

After the water maze test, mice were sacrificed and evaluated for changes in Aβ pathology using Thioflavin S staining. This demonstrated a dramatic reduction in Aβ deposition in both cortex and hippocampus of hUCB-MSC treated mice compared with PBS infused counterparts (Fig. 2A). Quantitative image analysis using the Metamorph 7.1.2 software confirmed this reduction as statistically significant for both the hippocampus and cortex ($p < 0.01$; Fig. 2B and 2C) in hUCB-MSC transplanted compared with PBS infused APP/PS1 mice. To confirm that the Thioflavin S results were a true reflection of quantitative change in brain Aβ protein levels, densitometric analysis of Aβ levels from western immunoblots was performed ($n = 5$ for each group). Western blotting with the 6E10 antibody, recognizing the APP and C-terminal fragments (CTFs), showed a decrease in the cortex and hippocampus of hUCB-MSC transplanted compared with the PBS injected animals (Fig. 2D, 2E). The reductions in Aβ were quantified and standardized according to the amount of β-actin protein, and were statistically significant ($p < 0.01$). The levels of Aβ 40 and 42 are elevated early in dementia, and this change has been strongly correlated with cognitive decline. Aβ 42 has been shown to be the most toxic Aβ isoform, and elicits an immunological response (Simard et al., 2006) and cognitive deficit (Koistinaho et al., 2001). To assess the relative contribution of Aβ isoforms to changes in total Aβ load, we further examined the brain sections with the isoform-specific Aβ 40 (G30) and Aβ 42 antibodies (20G10). In the hUCB-MSC treated group, the fraction of G30 (Fig. 3A and 3B) and 20G10 (Fig. 3E and 3F) positive plaques were dramatically lower than those in the PBS infused group. Quantitative image analysis showed that the area occupied by the Aβ40- and Aβ42-stained plaques was significantly smaller in the hUCB-MSC treated APP/PS1 mice than in their age-matched PBS infused counterparts ($p < 0.05$; figs 3C, 3D, 3G, and 3H). In addition, the deposition of Aβ 40 in the vascular wall was examined by double immunostaining with antibodies against α-smooth muscle actin (α vascular smooth muscle marker) and G30 (Skalli et al., 1986). We found that Aβ 40 was reduced in the vessels of APP/PS1 mice after hUCB-MSC treatment (Supplementary Fig. 1). We also analyzed cerebral Aβ 40 and 42 levels by Aβ sandwich ELISA ($n = 3$ for each group). Although there were no significant differences in Aβ levels detected by ELISA between the groups, we have found a trend toward a decrease of Aβ levels in hUCB-MSC treated APP/PS1 compared with PBS infused mice (Supplementary Fig. 2A and 2B). In addition, the results of immunohistochemistry and western blotting showed that hUCB-MSC transplanted mice had significantly lower levels of Aβ. Taken together, these observations suggest that hUCB-MSC transplantation was effective in reducing Aβ deposits. Furthermore, such an

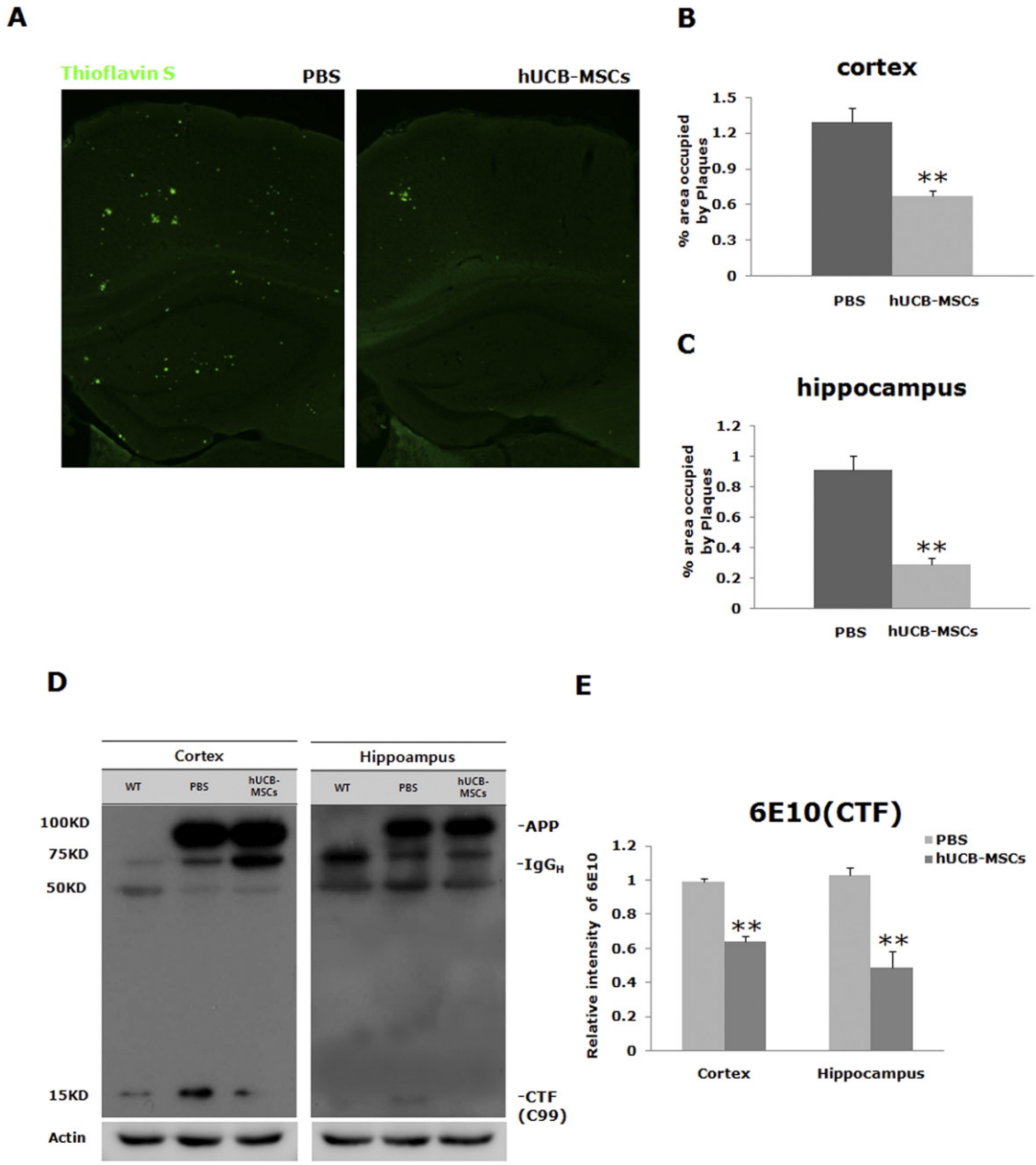

Fig. 2. hUCB-MSC treatment ameliorates Aβ plaques in the brains of APP/PS1 mice. (A) Brain sections from the cortex and hippocampus were stained with thioflavin S after hUCB-MSC or PBS treatment. Plaques are depicted by confocal microscopic images ($n = 5$ per group). (B and C) Quantitative image analysis representing the total % area of thioflavin S positive plaque burden, in the cortex (B) and hippocampus (C). The percentage area occupied by Aβ plaques was all reduced significantly in both the cortex and hippocampus of hUCB-MSC treated APP/PS1 mice compared with the PBS-infused mice. Data are expressed as mean ± SEM (Student's t-test); $n = 5$ for each group. (D and E) Protein content in the cortex and hippocampus of APP/PS1 mice after hUCB-MSC treatment ($n = 3$ per group) was analyzed by western blot using 6E10 antibody; values were normalized to actin levels. Values are mean ± SD. Student's t-test was used for statistical analysis. *$p < 0.05$ and **$p < 0.01$ compared with PBS infused APP/PS1 mice.

effect is sustained beyond the completion of the hUCB-MSC injection schedule.

Recent studies have shown that tau is a necessary component of Aβ-induced cognitive dysfunction in AD (Roberson et al., 2007), and that Aβ and tau are mechanistically linked (Blurton-Jones and Laferla, 2006). Our previous results (Fig. 2 and 3) indicated that hUCB-MSC transplantation reduced Aβ deposition including both aggregated Aβ 40 and 42 isoforms. Thus, we examined whether hUCB-MSC treatment likewise affected hyperphosphorylated tau pathology by immunostaining brain sections from PBS- or hUCB-MSC treated APP/PS1 mice and age-matched WT littermates with the AT8 antibody. hUCB-MSC treatment of APP/PS1 mice showed a significant reduction of hyperphos-

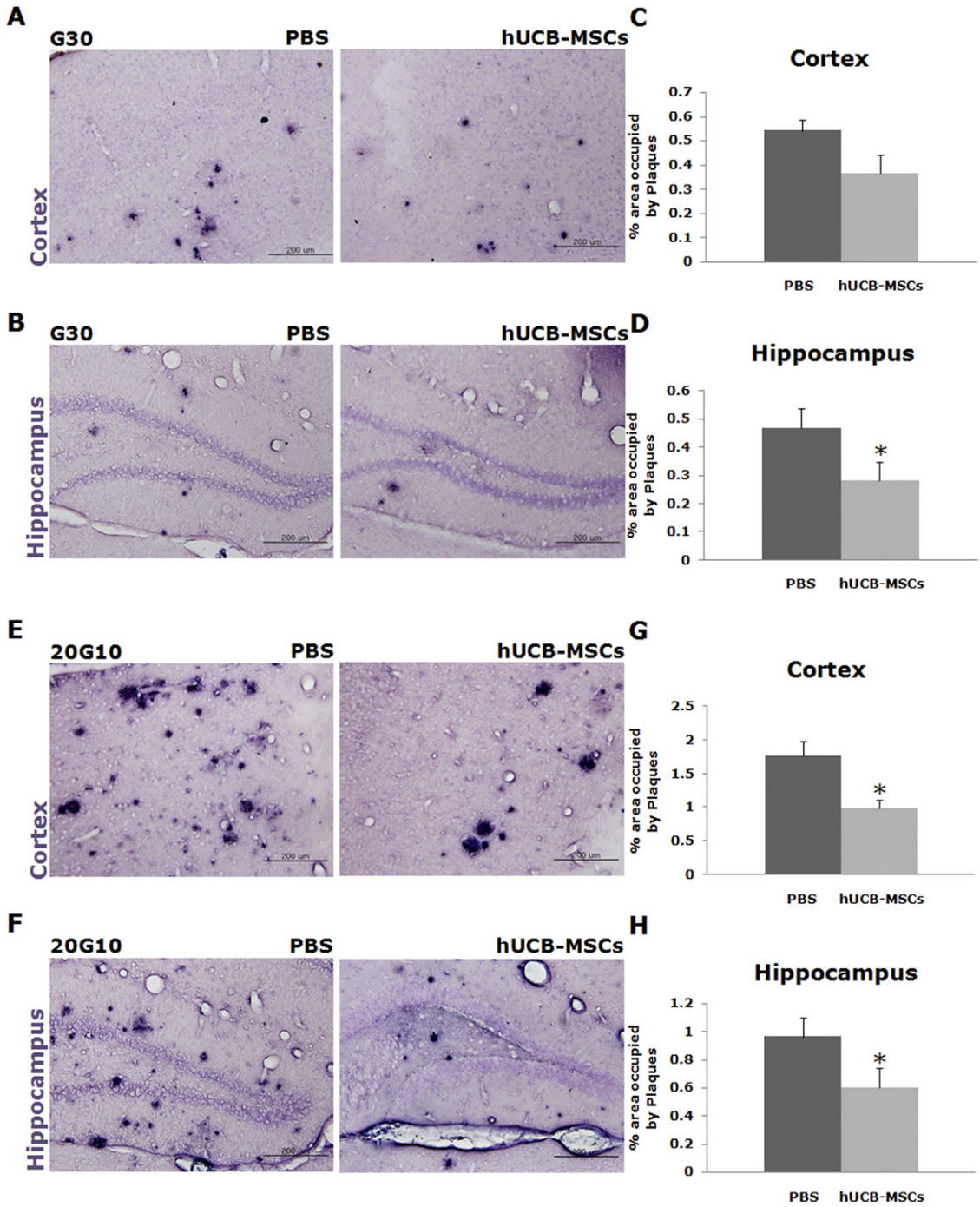

Fig. 3. hUCB-MSC treatment decreases Aβ 40 (G30, A and B), Aβ 42 (20G10, E and F) deposition in the cortex and hippocampus of APP/PS1 mice. Scale bars: 200 μm. Aggregated Aβ 40 (C and D) and 42 (G and H) were quantified by the percentage area of Aβ immunoreactivity. Values are mean ± SEM (Student's *t*-test. $n = 3$ for each group). *$p < 0.05$ compared with PBS treated APP/PS1 mice.

phorylated tau in the hippocampus and cortex compared with PBS controls (Supplementary Fig. 3).

2.3. hUCB-MSC treatment upregulates microglial activation in APP/PS1 mice

Cord blood cells have been shown to oppose the proinflammatory T_h1 response, as demonstrated in an animal model of stroke where cord blood cell infusion prompted a strong anti-inflammatory T_h2 response (Vendrame et al., 2004; Vendrame et al., 2005). Microglia are generally considered the immune cells of the CNS. Recently, we demonstrated that microglia are activated by bone marrow cell transplantation, and that these activated microglia decreased Aβ deposits in an acutely induced AD model (Lee et al.,

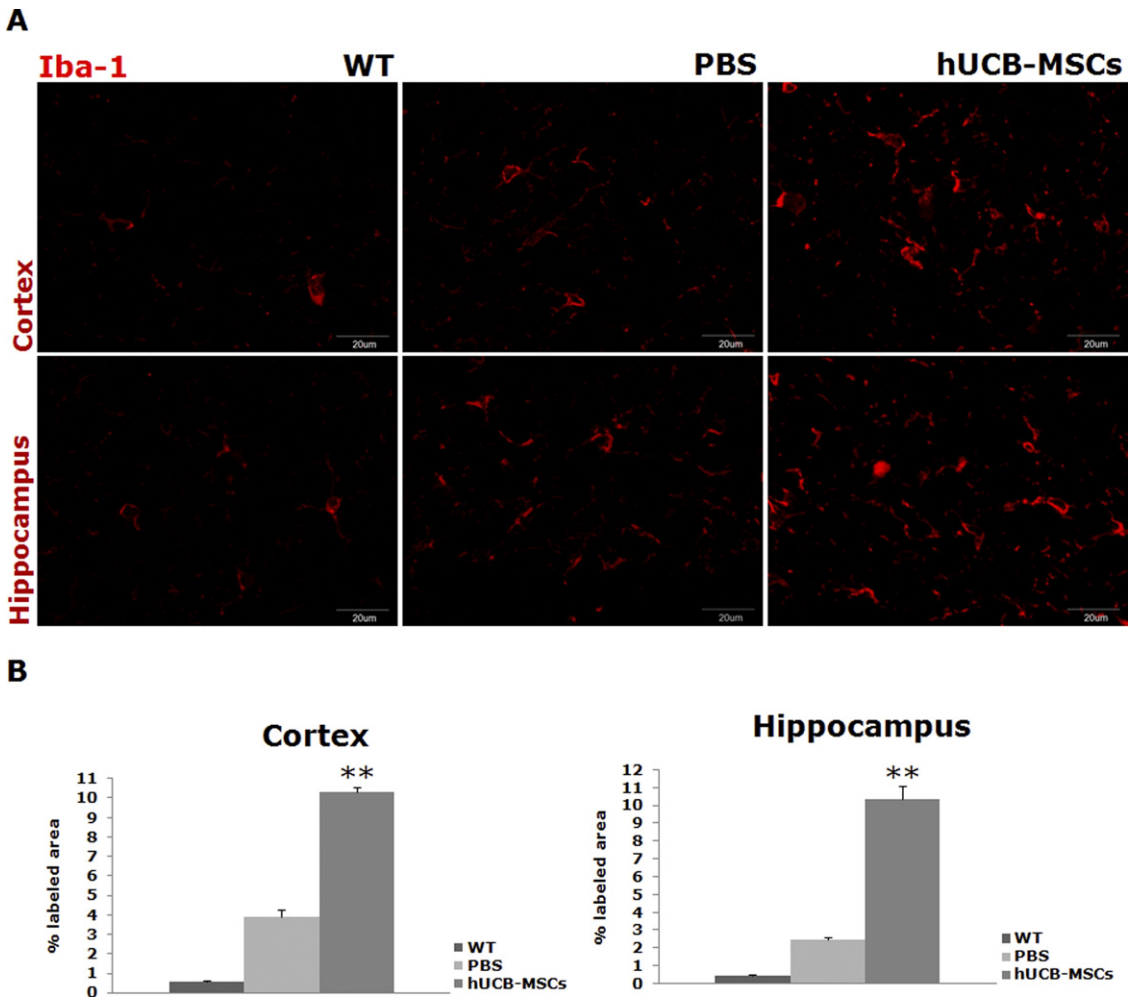

Fig. 4. hUCB-MSC transplantation triggers activation of the microglia in the cortex and hippocampus of APP/PS1 mice. (A) The general pattern of microglia in brain sections of PBS and hUCB-MSC treated APP/PS1 mice. $n = 3$ per group. Scale bar, 20 μm. (B) Quantitative image analysis of percent area of Iba-1$^+$ cells in the cortex and hippocampus of APP/PS1 mice treated with PBS and hUCB-MSC, respectively, is shown. Significantly increased Iba-1$^+$ cells were observed in the hUCB-MSC transplanted APP/PS1 mice compared with the PBS infused counterparts. Data represents mean ± SEM. ANOVA was used for statistical analysis. $^{**}p < 0.01$ compared with PBS infused APP/PS1 mice.

2009). Based on this and other previous reports, we examined whether hUCB-MSC transplantation can regulate microglia activity in the APP/PS1 mice. To investigate the number of activated microglia, brain sections were labeled using an Iba-1 antibody, and Iba-1 positive cells were increased to a greater extent in the cortex and hippocampus of hUCB-MSC treated APP/PS1 than PBS infused mice (Fig. 4A). Quantitative image analysis showed that the area occupied by Iba-1 was significantly increased in the hUCB-MSC treated APP/PS1 mice than in their age-matched PBS infused counterparts ($p < 0.01$; Fig. 4B). Thus, our results demonstrate that hUCB-MSC act to increase the population of microglia in the brains of APP/PS1 mice, and that this is not simply an effect of surgery or age. To validate whether the decreased Aβ deposition and increased microglia were stem cell-specific effect, we also transplanted NIH 3T3 cells into APP/PS1 mice. As expected, little effect was produced on Aβ deposits and microglia activation in NIH 3T3 cell-transplanted APP/PS1 mice. Indeed, results were similar to those of PBS infused APP/PS1 mice (data not shown). This result suggests that the reduction in Aβ deposition associated with increased microglia activation is specific for hUCB-MSC.

2.4. Decreased Aβ deposition following hUCB-MSC treatment is related to switching microglial phenotype from classic to the alternatively activated form

We next wanted to know the relationship between increased activated microglia and reduced Aβ load following transplantation of hUCB-MSC. Microglia secrete proteolytic enzymes that degrade Aβ, such as IDE (insulin-degrading enzyme), NEP (neprilysin), MMP-9 (matrix metalloproteinase 9), and plasminogen (Leissring et al., 2003; Yan et al., 2006). In addition, microglia also express receptors that promote the clearance and phagocytosis of Aβ,

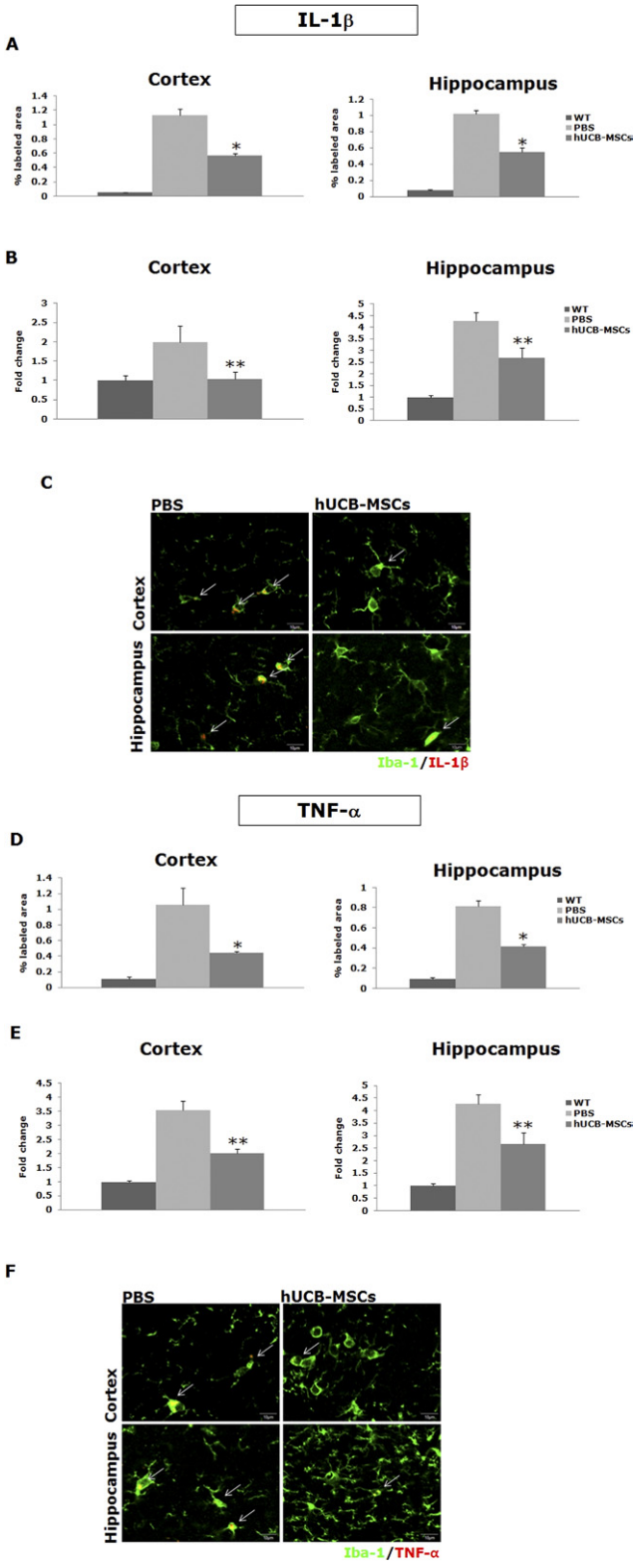

Fig. 5. Intrahippocampal hUCB-MSC treatment inhibits proinflammatory cytokines (IL-1β, and TNF-α) release from the activated microglia in the cortex and hippocampus of APP/PS1 mice. The quantitative image analysis of percent area of IL-1β (**A**) and TNF-α (D) in the cortex and hippocampus of APP/PS1 mice treated with PBS or hUCB-MSC and their age-matched, WT littermates, respectively, is shown. Data indicate mean ± SEM (ANOVA, Tukey's HSD test. $n = 4$ per group). The mRNA levels of IL-1β (B) and TNF-α (E) are measured. The expression of the different genes was normalized by β-actin. Expressions of these cytokines were increased in PBS-infused APP/PS1 mice compared with WT type. After hUCB-MSC treatment, there were significant decreases in RNA expression of both TNF-α and IL-1β. Data indicate mean ± SD (ANOVA, Tukey's HSD test. $n = 3$ per group). (C and F) Activated microglia (Iba-1 positive cells) by hUCB-MSC transplantation into APP/PS1 mice did not overlap in expression of both proinflammatory cytokine, IL-1β (C) and TNF-α (F) in the cortex and hippocampus of APP/PS1 mice. Scale bar, 10 μm. *$p < 0.05$ and **$p < 0.01$ compared with PBS infused APP/PS1 mice.

such as the Class A scavenger receptor, CD36, and the receptor for advanced-glycosylation endproducts (RAGE) (El Khoury et al., 1998; Yan et al., 1996). Therefore, we wondered whether the hUCB-MSC-specific effect on Aβ identified above might be mediated by modulating the expression of Aβ-degrading enzymes and Aβ-phagocytosis related receptors on microglia. To test this hypothesis, we measured expression of these proteolytic enzymes and receptors using quantitative real-time PCR analysis. There were no significant differences in expression of Aβ-binding phagocytic receptors (CD36, MARCO, SRB1, SRA, and RAGE) observed between the hUCB-MSC transplanted and PBS injected APP/PS1 groups (Supplementary Fig. 4A). mRNA expression levels of the Aβ-degrading enzymes NEP, IDE, and MMP-9 also were not changed in the brains of hUCB-MSC transplanted APP/PS1 mice (Supplementary Fig. 4B). These data demonstrate that the mechanism underlying the hUCB-MSC transplant effect on Aβ deposition in the APP/PS1 AD model excludes reversal of the disease-related decline in Aβ-degrading enzymes released by microglia and Aβ-phagocytosis related receptors on microglia.

The accumulation of Aβ in AD triggers increased expression of proinflammatory and potentially toxic cytokines released by activated microglia with tandem failure in their Aβ clearing activity (Heneka and O'Banion, 2007). The release of the proinflammatory cytokines, IL-1β and TNF-α, from neurotoxic microglia induces the production of Aβ and is related with neuronal dysfunction and cognitive impairments in AD. Indeed, downregulation of these cytokines has been shown to prevent neuronal dysfunction in AD (Halle et al., 2008; He et al., 2007). Thus, we examined expression of proinflammatory factors associated with increased Aβ deposition, IL-1β, TNF-α, and IL-6 in APP/PS1 mice compared with WT mice. As expected, quantitative image analysis confirmed that the levels of IL-1β and TNF-α were increased in the cortex and hippocampus of PBS infused APP/PS1 compared with WT mice ($p < 0.05$; Fig. 5A and 5D). In contrast, the levels of IL-1β and TNF-α were dramatically decreased in both the cortex and hippocampus of hUCB-MSC transplanted APP/PS1 animals compared with the PBS control. We also quantified the mRNA expression levels of IL-1β and TNF-α. Similarly, the expressions of IL-1β and TNF-α in the cortex and hippocampus of

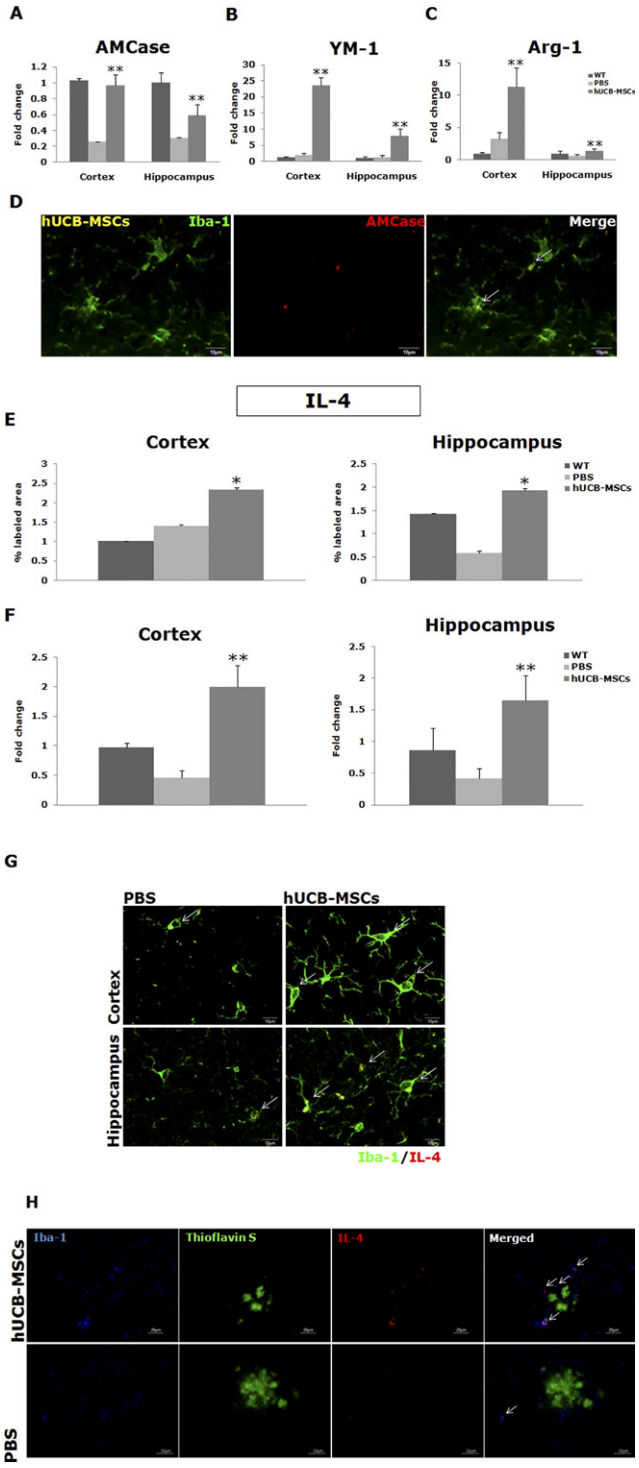

Fig. 6. hUCB-MSC treatment results in increased anti-inflammatory cytokine release from the alternative microglia phenotype in the cortex and hippocampus of APP/PS1 mice. (A, B, and C) mRNA expression of the alternative activation marker were quantitatively determined by real-time PCR in PBS and hUCB-MSC treated APP/PS1 mice. There were significant increases in RNA expression of AMCase, YM-1 and Arg-1 in hUCB-MSC transplanted APP/PS1 mice compared with PBS infused counterparts. Data indicate mean ± SD (ANOVA, Tukey's HSD test. $n = 3$ per each group). (D) Brain sections were stained with antibody against AMCase after hUCB-MSC treatment in APP/PS1 mice. The AMCase positive cells were colocalized predominantly with Iba-1 positive microglia in hUCB-MSC treated mice. Scale bar, 10 μm. (E) Brain section were stained with anti-inflammatory cytokine, IL-4 antibody and showed increase of IL-4 expression (E) after hUCB-MSC treatment compared with PBS infused mice. Quantitative image analysis of the total area of IL-4 positive cells, in the cortex and hippocampus. The percentage area occupied by IL-4 was increased significantly in both the cortex and hippocampus of hUCB-MSC treated APP/PS1 mice compared with the PBS infused mice. Data are expressed as mean ± SEM. (F) After hUCB-MSC treatment, there were significant increases in mRNA expression of IL-4 in APP/PS1 mice. Data are expressed as mean ± SD. ANOVA was used for statistical analysis ($n = 3$ per group). (G) Alternative microglia by hUCB-MSC transplantation was colocalized predominantly with anti-inflammatory cytokine, IL-4 in the cortex and hippocampus of APP/PS1 mice. (H) Triple labeling IL-4, thioflavin S, and Iba-1 in hUCB-MSC treated mice; demonstrated the existence of IL-4 positive microglia cell located near the Aβ plaques. Scale bar, 20 μm. *$p < 0.05$ and **$p < 0.01$ compared with PBS infused APP/PS1 mice.

PBS infused APP/PS1 mice as increased to a greater extent than WT mice, and the expression was reduced following intracerebral transplantation of hUCB-MSC ($p < 0.01$; Fig. 5B and 5E). The expression of IL-6 was not different between the groups (data not shown).

Next, to determine whether there was a reciprocal relationship between activated microglia and expression levels of proinflammatory cytokines in our treatment paradigms, we examined the relationship by double immunostaining with antibodies against IL-1β or TNF-α and Iba-1. Interestingly, we found that the number of Iba-1 positive cells expressing IL-1β or TNF-α was increased to a greater extent in cortex and hippocampus of PBS infused mice compared with hUCB-MSC transplanted APP/PS1 mice (Fig. 5C and 5F). It should also be noted that Iba-1 positive expression in the hUCB-MSC treated mice was higher than in control mice, confirming the observations described above (Fig. 4). Overall, the diminution in the expression of proinflammatory factors in the hUCB-MSC treated APP/PS1 mice occurred despite the apparent preservation of microglial activation. Thus, we hypothesized that the activated microglia in the hUCB-MSC treated animals had developed an alternative microglia phenotype more likely associated with anti-inflammatory effects. Alternatively activated microglia are commonly considered part of the repair process and extracellular matrix reorganization that begins during or after the first stages of an acute innate immune response (Gordon, 2003). It is well-established that IL-4 is associated with the alternative activation of the macrophage/microglia cell population (Colton et al., 2006; Gordon, 2003; Lyons et al., 2007). AMCase, YM-1 and Arg-1 are also strongly expressed in alternatively activated macrophages/microglia (Colton, 2009; Edwards et al., 2006; Lee et al., 2009; Matsumoto et al., 2009; Nair et al., 2005). To determine whether the activated microglia induced by hUCB-MSC treatment expressed alternatively activated microglia markers, we examined the expression of the AMCase, YM-1, Arg-1 and IL-4 genes. The results demonstrated a clear induc-

tion in the expression of AMCase, YM-1 and Arg-1 mRNA in the hUCB-MSC transplanted mice compared with the PBS infused group ($p < 0.01$; figs 6A, 6B, and 6C). Furthermore, we found that the AMCase expression in Iba-1 positive cells in hUCB-MSC treated APP/PS1 mice could be detected by immunostaining (Fig. 6D).

Using immunohistochemistry, the expression of IL-4 was also studied in hUCB-MSC and PBS infused APP/PS1 mice to further understand the colocation of alternatively activated microglia in relation to Aβ plaques. Immunohistochemistry showed that the level of IL-4 increased in APP/PS1 mice after hUCB-MSC transplantation ($p < 0.05$; Fig. 6E). Similarly, mRNA expression of IL-4 in the cortex and hippocampus of hUCB-MSC treated APP/PS1 mice also were increased compared with PBS infused mice ($p < 0.01$; Fig. 6F). Double immunofluorescence staining demonstrated that IL-4 expression in Iba-1 expressing cells was markedly increased in the cortex and hippocampus of hUCB-MSC transplanted APP/PS1 mice (Fig. 6G). Furthermore, triple labeling using antibodies against IL-4, Thioflavin S, and Iba-1 in hUCB-MSC treated mice, but not PBS infused mice, demonstrated the existence of IL-4 positive microglia cell located near the Aβ plaques (Fig. 6H). These results indicate that alternatively activated microglia surrounding Aβ plaques in the cortex and hippocampus of hUCB-MSC treated mice likely elicit a neuroprotective effect.

2.5. Immunomodulation regulates Aβ formation in APP/PS1 mice following hUCB-MSC treatment

Studies performed in transgenic animals suggest that neuroinflammation plays an important role in the process of cerebral amyloid deposition (Coraci et al., 2002; Lee et al., 2008). These and other studies also show that inflammatory cytokines such as IL-1β and TNF-α can augment Aβ formation (Blasko et al., 1999). It has been reported that cytokines are able to transcriptionally upregulate BACE-1 mRNA and protein (Sastre et al., 2003), and BACE-1 is a key rate-limiting enzyme that initiates Aβ formation (Vassar, 2001). To examine whether BACE-1 expression was affected by transplantation of hUCB-MSC into APP/PS1 mice compared with PBS infused mice, we studied BACE-1 levels in the cortex and hippocampus. These analyses found that BACE-1 levels in hUCB-MSC treated APP/PS1 mice were reduced in both western blot ($p < 0.05$; Fig. 7A and 7B) and real-time PCR ($p < 0.01$; Fig. 7C) compared with PBS injected animals.

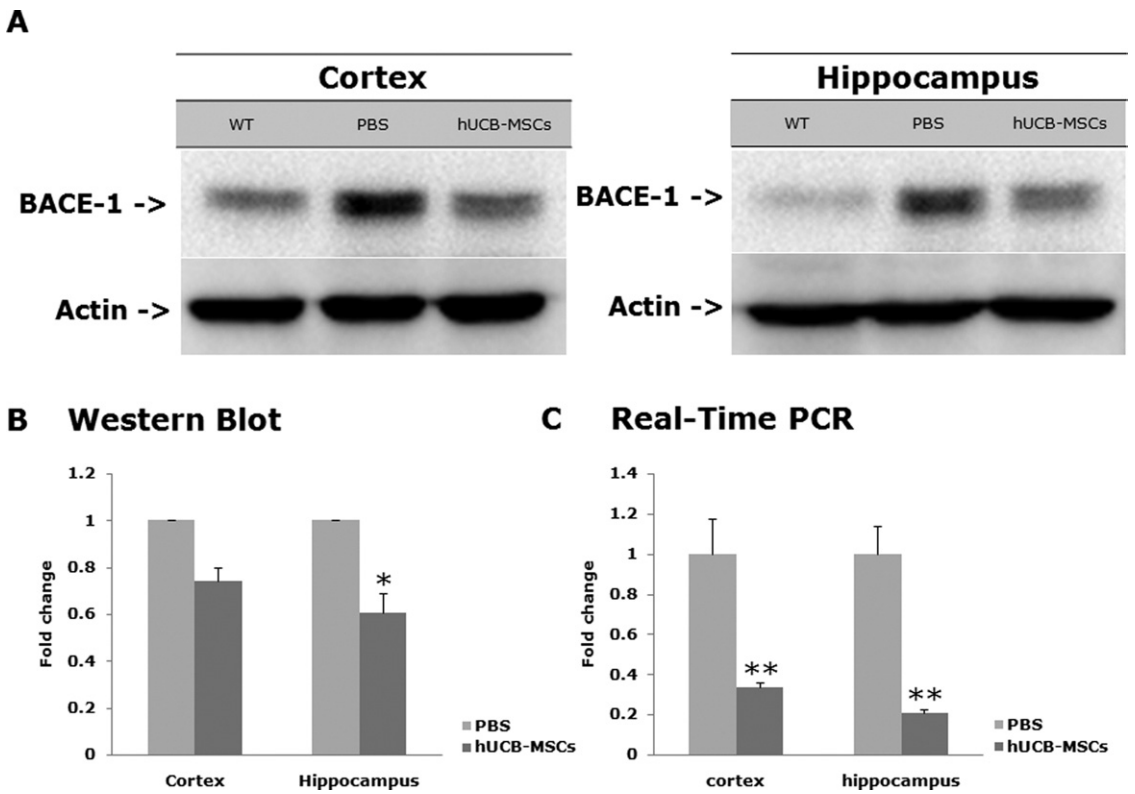

Fig. 7. Reduced inflammation response by hUCB-MSC transplantation downregulates BACE-1 expression (A) in the cortex and hippocampus of APP/PS1 mice. (B) Quantitative protein analysis of BACE-1 in the cortex and hippocampus of APP/PS1 mice. The BACE-1 expression was decreased significantly in both the cortex and hippocampus of hUCB-MSC treatment compared with the PBS infused mice. (C) BACE-1 mRNA levels were reduced significantly in hUCB-MSC transplanted APP/PS1 mice compared with PBS infused mice. Values were normalized to actin levels. Values are mean ± SEM. ANOVA was used for statistical analysis ($n = 3$ per group). *$p < 0.05$ and **$p < 0.01$ compared with PBS infused APP/PS1 mice.

3. Discussion

In the present study we used transgenic mice that overexpress the FAD-linked APP and PS1 transgenes to test the hypothesis that intracerebral hUCB-MSC transplantation would modulate Aβ deposition and cognitive decline *in vivo*. Clinicopathological studies in AD patients confirm that the hippocampus is one of the first regions of the brain where neuropathology appears. Thus, to maximize the efficacy of treatment, the hippocampus was chosen as the injection site for transplanted hUCB-MSC. We found that hUCB-MSC treatment was very effective in reducing Aβ deposits, and resulted in improved spatial learning and memory when compared with PBS infused APP/PS1 mice. Finally, the hUCB-MSC treated APP/PS1 mice exhibited decreased levels of neurotoxic cytokines associated with classically activated microglia, and increased levels of neuroprotective cytokines characteristic of alternatively activated microglia. Importantly, the alternatively activated microglia were also associated with Aβ plaques.

The effect of hUCB-MSC on reducing Aβ accumulation is likely attributable to inhibition of BACE-1 expression via immunomodulation. Amyloidogenic processing of the APP involves sequential cleavages by BACE-1 and γ-secretase at the N and C termini of Aβ, respectively. The 99-amino-acid C-terminal fragment of APP generated by BACE-1 cleavage can be internalized and further processed by γ-secretase to produce Aβ40/42. Several studies have indicated that neuroinflammatory reactions could contribute to BACE-1 expression (He et al., 2007; Lee et al., 2008; Sastre et al., 2003), and many also support the idea that neuroinflammation as a direct effect on Aβ formation (Blasko et al., 1999; He et al., 2007; Lee et al., 2008; Sastre et al., 2003). Our results demonstrated that BACE-1 expression decreased in hUCB-MSC treated APP/PS1 mice (Fig. 7A) through neuroinflammatory modulation, and that reduced expression of BACE-1 could diminish Aβ formation. Immunomodulation by hUCB-MSC treatment affects cytokine secretion from activated microglia. Activated microglia may play a critical role in AD by mediating Aβ processing. In these experiments, the number of Iba-1 positive microglia greatly increased in both cortex and hippocampus of hUCB-MSC treated compared with PBS infused APP/PS1 mice, with greater numbers in the hippocampus (Fig. 4). The diminution of Aβ plaque was also more significant in the hippocampus (Fig. 2). These differences may be attributable to a localized effect at the injection site. Concomitant with an elevated number of microglia, the area of Aβ plaques occupied by Aβ deposits were dramatically lower in the brains of hUCB-MSC treated mice (Fig. 2 and 3), and in most cases the plaques were smaller and less dense than those of PBS infused APP/PS1 mice. Also, the numbers of Iba-1 positive microglia that expressed anti-inflammatory cytokines were increased in response to hUCB-MSC transplantation (Fig 5 and 6). Taken together, our data confirms the established link between microglial activation and anti-inflammatory cytokines, and for the first time demonstrates that this can be specifically promoted via hUCB-MSC treatment in an AD model.

Activated microglia can adopt different phenotypes. Activated microglia in senile plaques has high expression of IL-1β and TNF-α (Halle et al., 2008). The aggregated Aβ protein, which is present in senile plaques of AD patients, activates microglia to produce neurotoxic substances that contribute to the neurodegenerative changes (Ponomarev et al., 2007). In neurological disorders, activated microglia are in a proinflammatory state (Clausen et al., 2008). Based on previous reports in AD patients and animal models, we wondered whether activated microglia induced by hUCB-MSC transplantation also produced proinflammatory cytokines. To examine this hypothesis, we studied the expression of TNF-α and IL-1β following hUCB-MSC treatment. The expression of TNF-α and IL-1β by both immunostaining and real-time PCR was significantly increased in 9 month old APP/PS1 mice compared with wild type mice. However, a remarkable decline in the expression of both TNF-α and IL-1β was detected in hUCB-MSC treated mice. This indicated that despite clear microglial activation in hUCB-MSC treated APP/PS1 mice compared with PBS infused animals (Fig. 5), the expression of cytotoxic proinflammatory factors was decreased. These results could be explained by the activated microglial cells adopting a different phenotype. Thus, we examined whether these activated microglial cells displayed a unique phenotype. Alternatively activated macrophages/microglia are primarily associated with wound healing and tissue repair (Colton et al., 2006; Gordon, 2003; Lyons et al., 2007). IL-4 is a well-described immune regulatory cytokine able to suppress inflammation (Colton et al., 2006; Falcone et al., 1998). The activation of microglia in the presence of IL-4 or IL-13 results in alternatively activated phenotype (Colton et al., 2006). In microglia, the alternative phenotype is characterized by the absence of expression of cytotoxic factors and the expression of alternative markers (AMCase, YM-1 and Arg-1) (Colton, 2009; Edwards et al., 2006; Lee et al., 2009; Matsumoto et al., 2009; Nair et al., 2005). Our results showed a clear induction in the expression of the IL-4, AMCase, YM-1 and Arg-1 genes in hUCB-MSC treated APP/PS1 mice compared with PBS infused APP/PS1 controls. Moreover, in the hUCB-MSC treated mice, immunostaining confirmed that IL-4 positive cells were localized predominantly around Aβ deposits, unlike in PBS infused mice, and were also colabeled with the activated microglia marker Iba-1. Therefore, our results suggest that the activated microglia induced by hUCB-MSC transplantation adopt an alternatively activated phenotype, and indicated that hUCB-MSC mediate their effects by inducing a neuroprotective phenotype in resident microglia. Many *in vitro* reports have probed the influence of IL-4 in the development of a non-proinflammatory alternative phenotype (Bu-

tovsky et al., 2006; Zhao et al., 2006). These studies demonstrate that in the presence of IL-4, microglia produce growth factors like IGF-1 (Koenigsknecht-Talboo and Landreth, 2005) and reduce Aβ toxicity, *in vitro* and *in vivo* (Butovsky et al., 2006; Zhao et al., 2006) and enhance Aβ phagocytosis (Butovsky et al., 2006). In our study, however, the expression of Aβ-degrading enzymes and Aβ-phagocytosis related receptors on microglia were not significantly different between the groups (Supplementary Fig. 4). Thus, our results confirm that the Aβ plaque-associated alternatively activated microglia induced by hUCB-MSC transplantation could reduce Aβ toxicity by increasing expression of IL-4, and was not a direct effect of enzymatic degradation or phagocytic activity.

Another interesting finding of the present study was the inhibition of tau hyperphosphorylation following hUCB-MSC transplantation. Recent evidence points to tau as a necessary component of Aβ-induced cognitive dysfunction (Blurton-Jones and Laferla, 2006; Roberson et al., 2007), suggesting that either a direct or indirect interaction between Aβ and tau may be central to the development of AD dementia. Despite the absence of human tau genes, the APP/PS1 transgenic mice used in these studies have previously been shown to accumulate small amounts of endogenous hyperphosphorylated mouse tau closely associated with Aβ plaques. Thus, we examined whether hUCB-MSC transplantation could reduce the levels of hyperphosphorylated tau. Indeed, hUCB-MSC transplantation of APP/PS1 mice showed a significant reduction of hyperphosphorylated tau in the hippocampus and cortex. The mechanisms behind the inhibitory role of hUCB-MSC on tau phosphorylation are largely unknown. However, in our experiments, reduced levels of endogenous phosphorylated tau after hUCB-MSC treatment may be related, at least in part, to decreased Aβ 42 levels produced by hUCB-MSC treatment. Excessive Aβ accumulation is associated with disturbed cognitive function as measured previously using a Morris water maze test in the APP/PS1 model and other transgenic models, and hyperphosphorylated tau leads to memory deficits and loss of functional synapses (Schindowski et al., 2006). In our mouse model, the PBS infused APP/PS1 mice took a significantly longer time to find the hidden platform than WT mice, indicating an impairment of spatial learning memory. When APP/PS1 mice were treated with hUCB-MSC, the latency was reduced (Fig. 1). These results suggest that hUCB-MSC treatment of the APP/PS1 mice significantly improves cognitive function. The beneficial effect of hUCB-MSC on cognition may be related to the combined effects of decreased levels of toxic Aβ peptide and tau hyperphosphorylation.

Recent observations indicate that the repair mechanism after tissue specific stem cell transplantation in brain diseases might be related to trophic mechanisms resulting in the release of bioactive factors (e.g. cytokines and growth factors), and by modulating the immune responses (Ding et al., 2007; Ohtaki et al., 2008). These and related results have focused attention on the paracrine effects of tissue specific stem cells such as hUCB-MSC (Ding et al., 2007), and are consistent with our results indicating that hUCB-MSC transplantation leads to activation of neuroinflammatory pathways.

In conclusion, our results strongly suggest that hUCB-MSC treatment reduces Aβ deposition and tau phosphorylation associated with the AD-like pathology in APP/PS1 mice. In addition, hUCB-MSC treatment prevented cognitive decline and memory impairment. When taken together, our results provide the basis for a novel immunomodulatory strategy for AD using hUCB-MSC.

Disclosure statement

The authors have no financial, personal, or other conflict of interest to disclose. Animal studies were performed with the approval of the Kyungpook National University Institutional Animal Care and Use Committee (KNU-IACUC), and all experiments were performed according to the guidelines of the KNU-IACUC. All efforts were made to minimize animal suffering and the number of animals used.

Acknowledgements

This research was supported by WCU (World Class University) program through the Korea Science and Engineering Foundation funded by the Ministry of Education, Science and Technology (R32-10064) and a grant (SC4170) from Stem Cell Research Center of the 21st Century Frontier Research Program funded by the Ministry of Science and Technology, Republic of Korea.

The first two authors contributed equally to this work.

Appendix. Supplementary data

Supplementary data associated with this article can be found, in the online version, at doi:10.1016/j.neurobiolaging.2010.03.024.

References

Blasko, I., Marx, F., Steiner, E., Hartmann, T., Grubeck-Loebenstein, B., 1999. TNFalpha plus IFNgamma induce the production of Alzheimer beta-amyloid peptides and decrease the secretion of APPs. FASEB J. 13, 63–68.

Blurton-Jones, M., Laferla, F.M., 2006. Pathways by which Abeta facilitates tau pathology. Curr. Alzheimer Res. 3, 437–448.

Butovsky, O., Koronyo-Hamaoui, M., Kunis, G., Ophir, E., Landa, G., Cohen, H., Schwartz, M., 2006. Glatiramer acetate fights against Alzheimer's disease by inducing dendritic-like microglia expressing insulin-like growth factor 1. Proc. Natl. Acad. Sci. U S A 103, 11784–11789.

Chen, S.H., Chang, F.M., Tsai, Y.C., Huang, K.F., Lin, C.L., Lin, M.T., 2006. Infusion of human umbilical cord blood cells protect against cerebral ischemia and damage during heatstroke in the rat. Exp. Neurol. 199, 67–76.

Clausen, B.H., Lambertsen, K.L., Babcock, A.A., Holm, T.H., Dagnaes-Hansen, F., Finsen, B., 2008. Interleukin-1beta and tumor necrosis factor-alpha are expressed by different subsets of microglia and macrophages after ischemic stroke in mice. J. Neuroinflammation 5, 46.

Colton, C.A., 2009. Heterogeneity of microglial activation in the innate immune response in the brain. J Neuroimmune Pharmacol. 4, 399–418.

Colton, C.A., Mott, R.T., Sharpe, H., Xu, Q., Van Nostrand, W.E., Vitek, M.P., 2006. Expression profiles for macrophage alternative activation genes in AD and in mouse models of AD. J. Neuroinflammation 27, 3, 27.

Coraci, I.S., Husemann, J., Berman, J.W., Hulette, C., Dufour, J.H., Campanella, G.K., Luster, A.D., Silverstein, S.C., El-Khoury, J.B., 2002. CD36, a class B scavenger receptor, is expressed on microglia in Alzheimer's disease brains and can mediate production of reactive oxygen species in response to beta-amyloid fibrils. Am. J. Pathol. 160, 101–112.

Ding, D.C., Shyu, W.C., Chiang, M.F., Lin, S.Z., Chang, Y.C., Wang, H.J., Su, C.Y., Li, H., 2007. Enhancement of neuroplasticity through up-regulation of beta1-integrin in human umbilical cord-derived stromal cell implanted stroke model. Neurobiol. Dis. 27, 339–353.

Duff, K., Eckman, C., Zehr, C., Yu, X., Prada, C.M., Perez-Tur, J., Hutton, M., Buee, L., Harigaya, Y., Yager, D., Morgan, D., Gordon, M.N., Holcomb, L., Refolo, L., Zenk, B., Hardy, J., Younkin, S., 1996. Increased amyloid-beta42(43) in brains of mice expressing mutant presenilin 1. Nature 383, 710–713.

Edwards, J.P., Zhang, X., Frauwirth, K.A., Mosser, D.M., 2006. Biochemical and functional characterization of three activated macrophage populations. J. Leukoc. Biol. 80, 1298–1307.

El Khoury, J., Hickman, S.E., Thomas, C.A., Loike, J.D., Silverstein, S.C., 1998. Microglia, scavenger receptors, and the pathogenesis of Alzheimer's disease. Neurobiol. Aging 19, S81–S84.

El Khoury, J.B., Moore, K.J., Means, T.K., Leung, J., Terada, K., Toft, M., Freeman, M.W., Luster, A.D., 2003. CD36 mediates the innate host response to beta-amyloid. J. Exp. Med. 197, 1657–1666.

Falcone, M., Rajan, A.J., Bloom, B.R., Brosnan, C.F., 1998. A critical role for IL-4 in regulating disease severity in experimental allergic encephalomyelitis as demonstrated in IL-4-deficient C57BL/6 mice and BALB/c mice. J. Immunol. 160, 4822–4830.

Games, D., Bard, F., Grajeda, H., Guido, T., Khan, K., Soriano, F., Vasquez, N., Wehner, N., Johnson-Wood, K., Yednock, T., Seubert, P., Schenk, D., 2000. Prevention and reduction of AD-type pathology in PDAPP mice immunized with A beta 1–42. Ann. N Y Acad. Sci. 920, 274–284.

Gordon, S., 2003. Alternative activation of macrophages. Nat. Rev. Immunol. 3, 23–35.

Halle, A., Hornung, V., Petzold, G.C., Stewart, C.R., Monks, B.G., Reinheckel, T., Fitzgerald, K.A., Latz, E., Moore, K.J., Golenbock, D.T., 2008. The NALP3 inflammasome is involved in the innate immune response to amyloid-beta. Nat. Immunol. 9, 857–865.

Harris, D.T., 2008. Cord blood stem cells: a review of potential neurological applications. Stem. Cell Res. 4, 269–274.

He, P., Zhong, Z., Lindholm, K., Berning, L., Lee, W., Lemere, C., Staufenbiel, M., Li, R., Shen, Y., 2007. Deletion of tumor necrosis factor death receptor inhibits amyloid beta generation and prevents learning and memory deficits in Alzheimer's mice. J. Cell Biol. 178, 829–841.

Heneka, M.T., O'Banion, M.K., 2007. Inflammatory processes in Alzheimer's disease. J. Neuroimmunol. 184, 69–91.

Hirko, A.C., Dallasen, R., Jomura, S., Xu, Y., 2008. Modulation of inflammatory responses after global ischemia by transplanted umbilical cord matrix stem cells. Stem Cells 26, 2893–2901.

Hsiao, K., Chapman, P., Nilsen, S., Eckman, C., Harigaya, Y., Younkin, S., Yang, F., Cole, G., 1996. Correlative memory deficits, Abeta elevation, and amyloid plaques in transgenic mice. Science 274, 99–102.

Huang, H.C., Jiang, Z.F., 2009. Accumulated amyloid-beta peptide and hyperphosphorylated tau protein: relationship and links in Alzheimer's disease. J. Alzheimers Dis. 16, 15–27.

Jimenez, S., Baglietto-Vargas, D., Caballero, C., Moreno-Gonzalez, I., Torres, M., Sanchez-Varo, R., Ruano, D., Vizuete, M., Gutierrez, A., Vitorica, J., 2008. Inflammatory response in the hippocampus of PS1M146L/APP751SL mouse model of Alzheimer's disease: age-dependent switch in the microglial phenotype from alternative to classic. J. Neurosci. 28, 11650–11661.

Kim, D.S., Kim, J.H., Lee, J.K.. Choi, S.J. Kim, J.S., Jeun, S.S., Oh, W., Yang Y.S., Chang. J.W., (2009). Overexpression of CXC chemokine receptors is required for the superior glioma-tracking property of umbilical cord blood-derived mesenchymal stem cells. Stem Cells and Development 18, 511–519.

Koenigsknecht-Talboo, J., Landreth, G.E., 2005. Microglial phagocytosis induced by fibrillar beta-amyloid and IgGs are differentially regulated by proinflammatory cytokines. J. Neurosci. 25, 8240–8249.

Koistinaho, M., Ort, M., Cimadevilla, J.M., Vondrous, R., Cordell, B., Koistinaho, J., Bures, J., Higgins, L.S., 2001. Specific spatial learning deficits become severe with age in beta -amyloid precursor protein transgenic mice that harbor diffuse beta-amyloid deposits but do not form plaques. Proc. Natl. Acad. Sci. U S A 98, 14675–14680.

Lee, C.G., Hartl, D., Lee, G.R., Koller, B., Matsuura, H., Da Silva, C.A., Sohn, M.H., Cohn, L., Homer, R.J., Kozhich, A.A., Humbles, A., Kearley, J., Coyle, A., Chupp, G., Reed, J., Flavell, R.A., Elias, J.A., 2009. Role of breast regression protein 39 (BRP-39)/chitinase 3-like-one in Th2 and IL-13-induced tissue responses and apoptosis. J. Exp. Med. 206, 1149–1166.

Lee, J.K., Jin, H.K., Bae, J.S., 2009. Bone marrow-derived mesenchymal stem cells reduce brain amyloid-beta deposition and accelerate the activation of microglia in an acutely induced Alzheimer's disease mouse model. Neurosci. Lett. 450, 136–141.

Lee, J.W., Lee, Y.K., Yuk, D.Y., Choi, D.Y., Ban, S.B., Oh, K.W., Hong, J.T., 2008. Neuro- inflammation induced by lipopolysaccharide causes cognitive impairment through enhancement of beta-amyloid generation. J. Neuroinflammation 5, 37.

Leissring, M.A., Farris, W., Chang, A.Y., Walsh, D.M., Wu, X., Sun, X., Frosch, M.P., Selkoe, D.J., 2003. Enhanced proteolysis of beta-amyloid in APP transgenic mice prevents plaque formation, secondary pathology, and premature death. Neuron 40, 1087–1093.

Livak, K.J., Schmittgen, T.D., 2001. Analysis of relative gene expression data using real-time quantitative PCR and the. 2 (-Delta Delta C(T)) Method. Methods 25, 402–408.

Lyons, A., Downer, E.J., Crotty, S., Nolan, Y.M., Mills, K.H., Lynch, M.A., 2007. CD200 ligand receptor interaction modulates microglial activation in vivo and in vitro: a role for IL-4. J. Neurosci. 27, 8309–8313.

Matsumoto, T., Inoue, H., Sato, Y., Kita, Y., Nakano, T., Noda, N., Eguchi-Tsuda, M., Moriwaki, A. Kan-O, K., Matsumoto, K., Shimizu, T. Nagasawa, H, Sakuda, S., Nakanishi, Y., 2009. Demethylallosamidin, a chitinase inhibitor, suppresses airway inflammation and hyperresponsiveness. Biochem. Biophys. Res. Commun. 390, 103–108.

Mattson, M.P., 2004. Pathways towards and away from Alzheimer's disease. Nature 430, 631–639.

Meda, L., Cassatella, M.A., Szendrei, G.I., Otvos, L., Jr, Baron, P., Villalba, M., Ferrari, D., Rossi, F., 1995. Activation of microglial cells by beta-amyloid protein and interferon-gamma. Nature 374, 647–650.

Morris, R.G., Garrud, P.. Rawlins, JN In O'Keefe, J., 1982. Place navigation impaired in. Rats with hippocampal lesion. Nature 297, 681–683.

Nair, M.G., Gallagher, I.J., Taylor, M.D., Loke, P., Coulson, P.S., Wilson, R.A., Maizels, R.M., Allen, J.E., 2005. Chitinase and Fizz family members are a generalized feature of nematode infection with selective upregulation of Ym1 and Fizz1 by antigen-presenting cells. Infect. Immun. 73, 385–394.

Nikolic, W.V., Hou, H., Town, T., Zhu, Y., Giunta, B., Sanberg, C.D., Zeng, J., Luo, D., Ehrhart, J., Mori, T., Sanberg, P.R., Tan, J., 2008. Peripherally administered human umbilical cord blood cells reduce parenchymal and vascular beta-amyloid deposits in Alzheimer mice. Stem Cells Dev. 17, 423–439.

Ohtaki, H., Ylostalo, J.H., Foraker, J.E., Robinson, A.P., Reger, R.L., Shioda, S., Prockop, D.J., 2008. Stem/progenitor cells from bone marrow decrease neuronal death in global ischemia by modulation of inflammatory/immune responses. Proc. Natl. Acad. Sci. U S A 105, 14638–14643.

Ponomarev, E.D., Maresz, K., Tan, Y., Dittel, B.N., 2007. CNS-derived interleukin-4 is essential for the regulation of autoimmune inflammation and induces a state of alternative activation in microglial cells. J. Neurosci. 27, 10714–10721.

Praticò, D., Trojanowski, J.Q., 2000. Inflammatory hypotheses: novel mechanisms of Alzheimer's neurodegeneration and new therapeutic targets? Neurobiol. Aging 21, 441–445.

Roberson, E.D., Scearce-Levie, K., Palop, J.J., Yan, F., Cheng, I.H., Wu, T., Gerstein, H., Yu, G.Q., Mucke, L., 2007. Reducing endogenous tau ameliorates amyloid beta-induced deficits in an Alzheimer's disease mouse model. Science 316, 750–754.

Sastre, M., Dewachter, I., Landreth, G.E., Willson, T.M., Klockgether, T., van Leuven, F., Heneka, M.T., 2003. Nonsteroidal anti-inflammatory drugs and peroxisome proliferator-activated receptor-gamma agonists modulate immunostimulated processing of amyloid precursor protein through regulation of beta-secretase. J. Neurosci. 23, 9796–9804.

Schenk, D., Barbour, R., Dunn, W., Gordon, G., Grajeda, H., Guido, T., Hu, K., Huang, J., Johnson-Wood, K., Khan, K., Kholodenko, D., Lee, M., Liao, Z., Lieberburg, I., Motter, R., Mutter, L., Soriano, F., Shopp, G., Vasquez, N., Vandevert, C., Walker, S., Wogulis, M., Yednock, T., Games, D., Seubert, P., 1999. Immunization with amyloid-beta attenuates Alzheimer-disease-like pathology in the PDAPP mouse. Nature 400, 173–177.

Schindowski, K., Bretteville, A., Leroy, K., Bégard, S., Brion, J.P., Hamdane, M., Buée, L., 2006. Alzheimer's disease-like tau neuropathology leads to memory deficits and loss of functional synapses in a novel mutated tau transgenic mouse without any motor deficits. Am. J. Pathol. 169, 599–616.

Simard, A.R., Soulet, D., Gowing, G., Julien, J.P., Rivest, S., 2006. Bone marrow-derived microglia play a critical role in restricting senile plaque formation in Alzheimer's disease. Neuron 49, 489–502.

Skalli, O., Ropraz, P., Trzeciak, A., Benzonana, G., Gillessen, D., Gabbiani, G., 1986. A Monoclonal Antibody against a-Smooth Muscle Actin: A New Probe for Smooth Muscle Differentiation. J. Cell Biol. 103, 2787–2796.

Tan, J., Town, T., Paris, D., Mori, T., Suo, Z., Crawford, F., Mattson, M.P., Flavell, R.A., Mullan, M., 1999. Microglial activation resulting from CD40·CD40L interaction after beta-amyloid stimulation. Science 286, 2352–2355.

Van Groen, T., Kadish, I., Wiesehan, K., Funke, S.A., Willbold, D., 2009. In vitro and in vivo staining characteristics of small, fluorescent, Abeta42-binding D-enantiomeric peptides in transgenic AD mouse models. Chemmedchem 4, 276–282.

Vassar, R., 2001. The beta-secretase, BACE: a prime drug target for Alzheimer's disease. J. Mol. Neurosci. 17, 157–170.

Vendrame, M., Cassady, J., Newcomb, J., Butler, T., Pennypacker, K.R., Zigova, T., Sanberg, C.D., Sanberg, P.R., Willing, A.E., 2004. Infusion of human umbilical cord blood cells in a rat model of stroke dose dependently rescues behavioral deficits and reduces infarct volume. Stroke 35, 2390–2395.

Vendrame, M., Gemma, C., de Mesquita, D., Collier, L., Bickford, P.C., Sanberg, C.D., Sanberg, P.R., Pennypacker, K.R., Willing, A.E., 2005. Anti-inflammatory effects of human cord blood cells in a rat model of stroke. Stem Cells Dev. 14, 595–604.

Wiley, C.A., Lopresti, B.J., Venneti, S., Price, J., Klunk, W.E., deKosky, S.T., Mathis, C.A., 2009. Carbon-11-labeled Pittsburgh Compound B and carbon-11-labeled (R)-PK11195 positron emission tomographic imaging in Alzheimer disease. Arch. Neurol. 66, 60–67.

Yan, P., Hu, X., Song, H., Yin, K., Bateman, R.J., Cirrito, J.R., Xiao, Q., Hsu, F.F., Turk, J.W., Xu, J., Hsu, C.Y., Holtzman, D.M., Lee, J.M., 2006. Matrix metalloproteinase-nine degrades amyloid-beta fibrils in vitro and compact plaques in situ. J. Biol. Chem. 281, 24566–24574.

Yan, S.D., Chen, X., Fu, J., Chen, M., Zhu, H., Roher, A., Slattery, T., Zhao, L., Nagashima, M., Morser, J., Migheli, A., Nawroth, P., Stern, D., Schmidt, A.M., 1996. RAGE and amyloid-beta peptide neurotoxicity in Alzheimer's disease. Nature 382, 685–691.

Zhao, W., Xie, W., Xiao, Q., Beers, D.R., Appel, S.H., 2006. Protective effects of an anti- inflammatory cytokine, interleukin-4, on motoneuron toxicity induced by activated microglia. J. Neurochem. 99, 1176–1187.